Title: Pubertal development and hypothalamic-pituitary-gonadal axis are altered in male mice lacking *Mecp2*

Authors: Ana Martín-Sánchez[1,2*#]; Daniela Jiménez-Díaz[1§]; Rafael Esteve-Pérez[1§], Alexandru Vasile-Tudorache[1]; Jordan E. Read[3]; Sasha R. Howard [3,4]; Carmen Agustín-Pavón[1*]

[1]Dept Cell Biology and Functional Biology, Faculty of Biological Sciences, Universitat de València, València, Spain

[2] Unitat Predepartamental de Medicina, Universitat Jaume I de Castelló, Castelló de la Plana, Spain

[3]Centre for Endocrinology, William Harvey Research Institute, Queen Mary University of London, London, UK

[4]Department of Paediatric Endocrinology, Royal London Children's Hospital, Barts Health NHS Trust, London, UK

[§] Equal contribution

*Corresponding authors

Ana Martín-Sánchez, anamarti@uji.es

Carmen Agustín-Pavón, m.carmen.agustin@uv.es

ORCID

Ana Martín-Sánchez 0000-0002-7046-8886

Daniela Jiménez-Díaz 0009-0000-2811-6134

Rafael Esteve-Pérez 0009-0004-6462-1604

Alexandru Vasile-Tudorache n/a

Jordan E. Read 0000-0001-6731-4440

Sasha R. Howard 0000-0002-6698-903X

Carmen Agustín Pavón 0000-0002-6725-6954

Statements

Availability of data

The datasets used and/or analysed during the current study are available from the corresponding author on reasonable request.

Funding

Funded by Ayudas FinRett 2022 and Subvenciones para grupos de investigación consolidados de la Conselleria de Educación, Cultura, Universidades y Empleo, Ref CIAICO/2023/027 to C.A.-P. SRH is funded by the Wellcome Trust (222049/Z/20/Z) and Barts Charity [MGU0552]. JER is funded by the British Society of Neuroendocrinology and the Society for Endocrinology. D.J.-D. is supported by a predoctoral fellowship from

Conselleria de Educación, Cultura, Universidades y Empleo, Generalitat Valenciana, ACIF/2024/402. R.E.-P. is supported by a predoctoral fellowship from Conselleria de Educación, Cultura, Universidades y Empleo, Generalitat Valenciana, ACIF/2022/387.

Conflict of interests

The authors declare that they have no conflict of interests

Ethics approval and consent to participate

All experimental procedures were approved by the Committee of Ethics and Animal Experimentation of the Universitat de València and treated according to the European Union Council Directive of June 3rd, 2010 (6106/1/10 REV1) and under an animal-usage license issued by the Direcció General de Producció Agrària i Ramaderia de la Generalitat Valenciana (2022/VSC PEA/0288).

Permission to reproduce material from other sources

Not applicable

Practical Applications

n/a

Authors' contributions

AMS performed experimental procedures, acquired images, analysed and interpreted data, prepared figures and wrote the manuscript; DJD, REP and AVT performed experiments and acquired images; JER contributed to data interpretation and writing; SRH obtained funding, designed the study, contributed to data interpretation and writing. CAP obtained funding, designed the study, performed and supervised experimental procedures, performed data analysis and wrote the manuscript. Final version of this manuscript was discussed and approved by all authors.

Acknowledgements

Authors are indebted to Paloma Sevilla-Ferrer and Carmen Tejada Cortés for technical assistance, to the personnel from the Animal Production and Experimentation of the Central Service for Experimental Research (SCSIE, UV) for their help with mice husbandry, to Dr Jose V. Torres-Pérez and Dr María Abellán-Álvaro for their help to set up the puberty measures, and to Prof. Fernando Martínez García, Dr MªJosé Sánchez Catalán and Prof. Enrique Lanuza for discussion of results.

Abstract

Background: Mutations in the *MECP2* gene, encoding the epigenetic reader Methyl-CpG binding protein 2, are the main cause of Rett syndrome, a rare neurodevelopmental disorder. Besides severe symptoms such as profound intellectual disability, loss of speech and motor skills and epilepsy, loss of function of *MECP2* has been associated with pubertal dysregulation, but the biological mechanisms leading to this remain unclear.

Methods: Using a mouse model of Rett, in which males are hemizygous and females heterozygous for *Mecp2* loss of function mutation, we assessed the onset and progression of puberty, together with increase in body weight and onset of neurological symptoms in post-weaning mice until puberty. In brain samples of young adult mice, we analysed hypothalamic Gonadotropin releasing hormone (GnRH) neurons by immunofluorescent labelling, and in plasma samples measured circulating GnRH, LH and testosterone concentrations. Finally, we analysed testosterone dependent arginine-vasopressin circuits.

Results: In our mouse model we found delayed puberty in *Mecp2* ^{CD1}-null males, associated with a reduced rate of weight gain, but with puberty onset occurring at a lower body weight than in wildtype controls. Despite later puberty onset, *Mecp2*^{CD1}-null male mice were found to have an increased number of GnRH neurons, but displayed lower levels of circulating reproductive hormones. Consequently, *Mecp2*^{CD1}-null males have deficient testosterone-dependent arginine-vasopressin innervation. In female *Mecp2*^{CD1}-heterozygous mice, we found no overall significant differences in pubertal development or GnRH neurons. The lack of significant alterations in females might be related to a later onset of neurological symptoms due to heterozygosity.

Conclusions: Our data supports that *MECP2* is essential for typical pubertal development, with complete loss of *Mecp2* in a male murine model resulting in abnormalities of pubertal timing related to lower body weight, with an observed increase in hypothalamic GnRH neurons.

Keywords

Gonadotropin-releasing hormone, *MECP2*, puberty, Rett syndrome, testosterone

Introduction

The X-linked *MECP2* gene encodes the methyl CpG-binding protein 2 (MeCP2), a multifunctional protein first characterised as a transcriptional repressor able to bind to methylated DNA (1) and currently mostly defined as an epigenetic reader with both transcriptionally repressive and activating functions (2) MeCP2 is expressed in a variety of tissues, but it has a fundamental role in the brain, where it is involved in the maintenance of a mature neuronal phenotype (3,4). Thus, mutations in *MECP2* are associated with several neurological disorders (5). In particular, loss of function mutations in *MECP2* are the main cause of Rett syndrome (RTT) (6), a rare neurodevelopmental disorder and one of the most severe conditions linked to this gene. RTT mainly affects girls, who are heterozygous for the mutation; on the contrary, boys suffer a complete loss of *MECP2* and typically die perinatally (5). Girls with RTT, who are born apparently healthy, develop the first symptoms around 6-18 months of age, including an arrest of development followed by loss of acquired skills. The main symptoms are loss of speech, loss of purposeful use of the hands, intellectual disability, epilepsy and progressive loss of ambulation (7). On the other hand, duplication of *MECP2,* causing duplication syndrome (MDS), affects boys, leading also to intellectual disability, motor impairment and epilepsy (7).

In addition to these severe symptoms, loss of function of *MECP2* can lead to endocrine dysregulation, which can contribute to emotional symptoms (8), and disordered puberty (9). Related to this, a handful of studies have reported cases of patients with RTT or MDS that display precocious puberty (10–12). Recently, rare variants of *MECP2* were identified in patients with central precocious puberty with isolated neurodevelopmental features, including autism or microcephaly, but without RTT (13,14). Further, pubertal trajectories have been seen to be altered in a subset of patients with RTT, with around 20% of females experiencing precocious onset of puberty but delayed menarche (9). This extended course of puberty, with early breast development but late pubertal completion, is also observed in disrupted oestrogen signalling such as from exposure to estrogenic endocrine-disrupting chemicals (15).

The onset of puberty is triggered by the activation of hypothalamic neurons containing Gonadotropin Realising Hormone (GnRH) (16). These neurons are neuroendocrine cells that develop within the nasal placode and reside in the olfactory bulbs, septum and the preoptic and anterior regions of the hypothalamus in the adult mammalian brain (17) . GnRH hypothalamic neurons, via pulsatile GnRH signalling, regulate the gonadotrope cells of the hypophysis, which release luteinizing hormone (LH) and follicle-stimulating hormone (FSH). In turn, LH and FSH control the production and release of gonadal

135 hormones (oestradiol, testosterone), which provide negative (and positive) feedback
136 signalling to the hypothalamus-pituitary to coordinate pubertal development and adult
137 reproduction.

138 Several potential pathways exist via which *MECP2* could influence GnRH activation.
139 Firstly, by means of its transcriptional control of FXYD domain-containing transport
140 regulator 1 (*FXYD1*), a protein responsible for control of GnRH neuronal excitability.
141 Patients with RTT and *Mecp2*-null mice demonstrate a pathogenic overexpression of
142 *FXYD1* in the frontal cortex of the brain, attributed to lack of repression by *MECP2* (18),
143 and mRNA levels of *Fxyd1* in rat brain closely correlate with increased GnRH neuron
144 excitability at puberty and first oestrus (19). Next, as an epigenetic regulator, MeCP2
145 regulates gene expression through interaction with both 5-methylcytosine (5mC) and 5-
146 hydroxymethylcytosine (5hmC) residues in DNA, impacting chromatin accessibility,
147 recruiting histone modifying enzymes and forming part of various polycomb complexes
148 (20–22). Beyond the traditional idea of MeCP2 as a repressor of gene expression
149 through its association with 5mC, it has also been found to associate with active
150 chromatin regions, enriched at 5hmC *loci* in neurons. The Rett syndrome *MECP2* variant
151 p.R133C preferentially disrupts the association with 5hmC (22). Likewise, MeCP2 has
152 demonstrated a strong co-localisation within the mouse cortex with repressing histone
153 mark H3K27Me3 (21) as well as an association with the activating histone mark
154 H3K4Me3 (20), indicating a role as both an activator and repressor of gene expression.
155 Additionally, evidence for estrogen receptor α and β (Erα and Erβ) expression in murine
156 GnRH neurons suggests a direct role for estrogen signalling in the regulation of GnRH
157 secretion (23). MeCP2 is seen to associate with the Erα promoter in mouse cortex,
158 correlating with increased promoter methylation and reduced Erα expression beyond
159 postnatal day 10 (P10). Female mutant *Mecp2* mice demonstrate an increase in this Erα
160 expression beyond P10, inverse to the reduced levels seen in wildtype mice, suggesting
161 a mis-regulation of Erα expression upon loss of functional *Mecp2* (24).
162 *Mecp2*-mutant mice are valuable model systems for the study of RTT (25). Loss of
163 function mutation is not immediately lethal to males, so *Mecp2*-null male mice survive
164 into young adulthood, albeit developing severe motor impairment and reduced lifespan
165 (25), and early onset of symptoms (26) The onset of symptoms in *Mecp2*-heterozygous
166 females is variable, with some of them displaying mild behavioural symptoms at young
167 age and others remaining pre-symptomatic until 4-6 months of age (8,27). Aside from
168 the typical motor symptoms, in the first report describing the model, Guy and
169 collaborators (25) noted that *Mecp2*-null males had universally undescended testicles
170 and were infertile. However, it is unclear whether males are unable to mate because of

171 their motor impairment, whether they exhibit inappropriate sexual behaviour or display
172 hormonal deficits. Young adult *Mecp2*-null males displayed low levels of testosterone-
173 dependent features, such as aggression, arginine-vasopressin (AVP) sexually dimorphic
174 central circuits and production of male pheromones (28). These data strongly suggest
175 that *Mecp2*-mutant mice could help to understand the mechanisms of altered pubertal
176 development observed in patients, but, to our knowledge, this has not been previously
177 investigated.
178 Thus, in this study, we sought to characterize the pubertal trajectories, analyse GnRH
179 neuronal circuitry and the levels of circulating sex hormones in a relatively novel model
180 of *Mecp2* mutant mice on CD1 background (29) .
181
182 **Material and methods**
183 ***Animals and rearing conditions***
184 For this study, we crossed *Mecp2*-heterozygous females bred in-house (B6.129P2(C)-
185 Mecp2$^{tm1.1Bird/J}$, The Jackson Laboratory) with pure CD1 males (Crl:CD1(ICR), Charles
186 River Laboratories) for more than 10 generations, to ensure complete derivation to the
187 CD1 strain, as per (29). Our decision to derive the model to CD1 background was in
188 order to maximize colony productivity while maintaining the disease phenotype (27).
189 Moreover, a relatively recent systematic review found that, contrary to conventional
190 assumptions, the use of outbred mice, such as CD1, might be preferrable to the use of
191 inbred strains for biomedical research (30) Animals were housed with *ad libitum* water
192 and food in a room maintained at 22 ± 1ºC, humidity 55 ± 10% and a12:12 h light/dark
193 cycle, with lights on at 08:00h. All experimental procedures were approved by the
194 Committee of Ethics and Animal Experimentation of the Universitat de València and
195 treated according to the European Union Council Directive of June 3rd, 2010 (6106/1/10
196 REV1) and under an animal-usage license issued by the Direcció General de Producció
197 Agrària i Ramaderia de la Generalitat Valenciana (2022/VSC PEA/0288).
198 ***Genotyping and expression of MeCP2 in the brain***
199 For genotyping, we obtained ear biopsies at weaning and after DNA extraction we
200 applied the protocol supplied for this strain by the Jackson Laboratory. To further assess
201 the loss of MeCP2 protein expression in the new strain, we carried out an
202 immunofluorescent detection of MeCP2 in a WT and *Mecp2*^{CD1}-null males
203 (Supplementary material, Figure S1).
204 ***Assessment of reproductive capacity of Mecp2^{CD1}-het females***
205 To assess whether *Mecp2*^{CD1}-het females displayed typical breeding, we recorded the
206 time lapse in days since pairing with a stud male until first delivery, and the number of
207 pups surviving until weaning age (postnatal day 23) in the first litter, at F0, F1, F2, F3 in

208 the original *Mecp2*^{Bird}-het strain (n=17), and at the F0, F1, F2, F3, and F9, F10 and >F10
209 in the *Mecp2*^{CD1}-het females (n=28). Breeding pairs consisted in one-two young adult
210 *Mecp2*-het females (7-8 weeks of age) plus one stud male from the pure C56/BL6J (Bird
211 strain) or CD1 (CD1 strain) background.

212 ***Weight gain, puberty onset and oestrous cycle monitoring***

213 All mice were weaned at P23. Mice were weighed daily the first week after weaning, from
214 P25 to P31, to monitor weight gain due to its influence on the onset of puberty (females,
215 WT, n= 16, *Mecp2*^{CD1}-het, n=11; males: WT, n=16; *Mecp2*^{CD1}-null, n=21). Mice that
216 achieved vaginal opening or balanopreputial separation after P31 were weighed daily
217 until the day that puberty parameter was achieved. Puberty was determined by the day
218 of vaginal opening in females and balanopreputial separation in males, respectively, from
219 postnatal day 25 (P25) (females, WT, n = 23, *Mecp2*^{CD1}-het, n = 16; males: WT, n =16;
220 *Mecp2*^{CD1}-null, n =21) (31,32). Balanopreputial separation in males was assessed by
221 gently attempting manual retraction of the prepuce. Additionally, we determined the
222 occurrence of the first oestrous in a subset of those females by collecting vaginal smears
223 from the day of vaginal opening until first oestrous (WT, n = 10; *Mecp2*^{CD1}-het, n = 10),
224 and oestrous cyclicity in a subset of the females by monitoring the duration of the phases
225 of the oestrus cycle for 10 days after P35 (WT, n = 12; *Mecp2*^{CD1}-het, n = 8). Briefly,
226 vaginal cells were collected by gently flushing the external vaginal area with a small
227 amount (50-100 µl) of saline solution (NaCl 0.9%, Braun), using a pipette inserted into a
228 sterile latex bulb. The liquid was slowly released into the vaginal opening and then drawn
229 back into the pipette using the bulb. The process was repeated 4-5 times using the same
230 solution until the resulting fluid became turbid. Then, the solution with cell suspension
231 was dropped over a glass slide, dried using a hot plate, and counterstained using a
232 toluidine blue (Sigma-Aldrich) 0.25% solution (33).

233 ***Perfusion, fixation and tissue sectioning***

234 At two months old, an age considered in mice as young adulthood with full reproductive
235 capacity (34), animals (females, WT, n = 6, *Mecp2*^{CD1}-het, n = 6; males: WT, n = 5-6;
236 *Mecp2*^{CD1}-null, n = 6-7) were deeply anaesthetized using a dolethal overdose (i.p.
237 injection of 0.02 mg/g of body weight of pentobarbital-based solution). Then, animals
238 were euthanized by transcardial perfusion of phosphate saline solution 0.1 M (PBS 0.1M,
239 pH 7.4) using a peristaltic pump (5.5 ml/min for 2 min) followed by 4% paraformaldehyde
240 in 0.1 M PBS, pH 7.4 (same flux for 5 min). Brains were carefully removed and
241 immediately post-fixed in the same fixative solution overnight at 4ºC. Then, brains were
242 cryoprotected (30% sucrose solution in 0.1 M PBS, pH 7.6, 4ºC) and cut into five sets of
243 40µm-thick coronal sections using a freezing microtome (Leica SM 2010R) and stored
244 with 30% sucrose and 0.02% sodium azide in 0.1 M PB at -80ºC. In another subset of

245 mice (females, WT, n = 3, *Mecp2*^{CD1}-het, n = 3; males: WT, n=5; *Mecp2*^{CD1}-null, n=5),
246 gonads were removed, postfixed in PFA 4% and stored with 70% ethanol solution,
247 included in paraffin, sectioned in 10 µm-thick sections and counterstained with
248 haematoxylin-eosin.
249
250 ***Immunofluorescence for GnRH and AVP***
251 We performed GnRH immunofluorescence in one of the five parallel coronal series from
252 both sexes and genotypes (WT females n= 6; Mecp2CD1-het n = 6; WT males n = 5,
253 Mecp2CD1-null n = 7), and AVP immunofluorescence in another brain series, only from
254 males, from both genotypes (WT n = 6, *Mecp2*^{CD1}-null n = 6). Briefly, free-floating
255 sections were washed with 0.05 M TRIS buffered saline pH 7.6 (TBS) (3 × 10 min). Then,
256 sections were: (i) pre-incubated in 3% normal donkey serum (NDS; Sigma-Aldrich,
257 G9023) in TBS with 0.2% Triton X-100, at RT for 1 h, to block non-specific labelling; (ii)
258 incubated with TBS with 0.3% Triton X-100, 2% NDS for 48 h at 4 °C with monoclonal
259 rabbit anti-GnRH primary antibody (1:5000, Invitrogen, AB1567) or rabbit anti-
260 vasopressin IgG (1:1000; Chemicon, AB1565); (iii) incubated with fluorescent-labelled
261 RedTM-X-conjugated at a 1:500 dilution (Jackson ImmunoResearch, 711- 295-152)
262 secondary antibody (90 min at RT) diluted in TBS. To reveal the cytoarchitecture in brain
263 sections, they were counterstained prior to mounting by 5 min washes in 4',6- diamino-
264 2-feniindol (DAPI, a nuclear staining) at a 1:10000 dilution. After each step, sections
265 were washed 3 times for 5 min in TBS except between step (ii) and (iii). Finally, sections
266 were rinsed thoroughly in TB, mounted onto gelatinised slides and cover-slipped with
267 fluorescence mounting medium FluorSave Reagent (Sigma-Aldrich, 345789).
268 ***Determination of circulating hormonal levels***
269 Blood samples from young adult male mice (WT, n = 5-15; *Mecp2*^{CD1}-null, n = 9-13) were
270 obtained from the aortic arch immediately before perfusion (between 10:00 a.m. and
271 13:00 a.m.) and under anaesthesia conditions. These samples were collected into
272 heparinized tubes, which were rapidly centrifuged at 20.000 g for 15 min at RT
273 (Eppendorf 5424 Centrifuge), until plasma was separated from blood cells. Supernatant
274 (100 µl) was collected and immediately stored at -80C until used. Samples selected for
275 ELISA were processed according to the protocol supplied by the ELISA kit manufacturer
276 for testosterone (Bio-Techne R&D Systems, S.L.U. KGE010), LH (Fine Test, EM1188)
277 and GnRH (ElabScience, E-EL-0071) determination. Optical density was read at 450 nm
278 in a Thermo Scientific Multiskan FC automatic spectrophotometer. Concentrations were
279 calculated using their standard curves.
280 ***Microscopy and image acquisition***

281 Brain and gonadal samples were analysed using a microscope equipped with light and
282 fluorescent lamps (Leica Microsystems series 140269 LEITZ DMRB microscope, digital
283 camera LEICA DFC495). Fiji-ImageJ software was employed to manually quantify the
284 number of follicles and corpora lutea, spermatids and Leydig cells, GnRH-positive and
285 AVP-ergic cells using the *cell counter* plugging. In gonadal samples, number of elements
286 are normalized by the area of the sample, and in brain samples this number is relative
287 to the number of slices containing the area o interest. For AVP-ergic innervation, we
288 quantified the area fraction occupied by AVP-immunoreactive pixels in the image after
289 appropriate thresholding. No manipulations of individual image elements were carried
290 out.

291 ***Statistical analysis***

292 Data were analysed using IBM SPSS Statistics 23.0 and GraphPad Prism. We first
293 checked the data for normality (Kolmogorov-Smirnov's test) and homoscedasticity
294 (Levene's test). We performed Student's t-test, one-way ANOVAs and ANOVA for
295 repeated measurements to analyse the weight variation across different ages. Kaplan-
296 Meier analysis was used to evaluate differences in the observation of vaginal opening,
297 first oestrous in females and balanopreputial separation in males. When applicable,
298 pairwise comparisons were analysed with Bonferroni's correction. When data were not
299 normally distributed, Mann-Whitney's test was used for the number of follicles data.
300 Statistical differences were considered significant when $p < 0.05$.

301

302 **Results**

303 ***Mecp2^{CD1}*-het females provide larger litters than *Mecp2^{Bird}*-het females, while**
304 **maintaining the neurological phenotype**

305 We first analysed whether reproductive capacity was increased in the *Mecp2*^{CD1}-het
306 females, as previously reported (35). In the number of days from pairing with a stud male
307 until delivery of the first litter we found no significant differences between strains (Mann-
308 Whitey test, $p > 0.05$, Supplementary material, Figure S2A). By contrast, the number of
309 pups surviving until weaning in the first litter was significantly higher in the *Mecp2*^{CD1}-het
310 as compared to *Mecp2*^{Bird}-het females (Mann-Whitney test, $p < 0.01$, Supplementary
311 material, Figure S2B).

312 **Pubertal development of *Mecp2^{CD1}*-het females is not significantly different from**
313 **WT controls**

314 The weight of female *Mecp2^{CD1}*-het mice increased across days during the first week
315 post-weaning (repeated measures ANOVA, $F_{3,23} = 3.95$ $p < 0.001$, Figure 1a), with no
316 differences compared to WT controls. Similarly, no significant differences in timing of
317 vaginal opening (Kaplan-Meier analysis, $p > 0.05$, Figure 1b) or weight at first oestrous

318 (Student's t-test, p > 0.05, Figure 1c) were observed between *Mecp2*^{CD1}-het females and
319 their WT counterparts. Further, we found no significant differences between genotypes
320 in the occurrence of first oestrous, that happened 2.8±0.7 days after vaginal opening in
321 WT and 2.6±0.7 days after vaginal opening in *Mecp2*^{CD1}-het females (Kaplan-Meier
322 analysis, p > 0.05, Figure 1d), cycle length and oestrous cyclicity for ten days from P35
323 to P45 (Student's t-test, p > 0.05 in both cases, Figure 2e, f, and Supplementary Figure
324 S3). Finally, histological analysis of the ovaries revealed the presence of follicles in all
325 phases of development, with no significant differences in the number of follicles in any
326 phase (Mann-Whitney rank test, p > 0.05, Figure 1g) and no histological abnormalities
327 (Figure 1h and h').

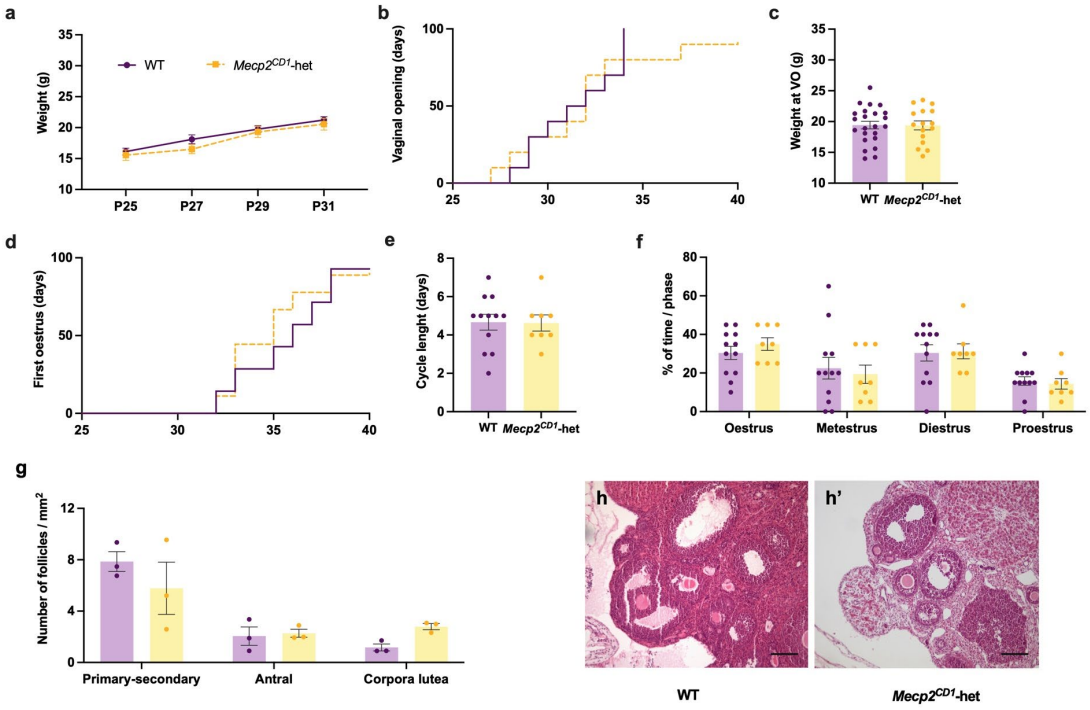

328

329 **Figure 1. Weight gain, pubertal development, and histology of the ovaries are not**
330 **significantly affected in *Mecp2*^{CD1}-het female mice.** a) Graphical representation of
331 body weight gain in *Mecp2*^{CD1}-het females in comparison with their WT control mice. b)
332 Days to vaginal opening. c) Weight at vaginal opening. d) Days to first oestrous. e) Cycle
333 length (oestrous to oestrous) and (f) percentage of time in each phase of the oestrous
334 cycle across 10 days of monitoring. g) Number of follicles in different stages. f)
335 Histological images of representative WT (h) and *Mecp2*^{CD1}-het (h') ovaries. Data are
336 shown as Mean ± S.E.M. Scale bar: 50µm

337

338 **Puberty is significantly delayed in *Mecp2*^{CD1}-null males and associated with lower**
339 **weight**

The weight of *Mecp2*^{CD1}-null males was significantly lower during the first week post-weaning as compared to WT males (repeated measures ANOVA, $F_{1,35} = 15.76$, $p < 0.001$, Figure 2a). The onset of puberty of *Mecp2*-null males showed a significant delay when compared to WT animals (Kaplan-Meier, $\chi^2 = 6.025$, df = 1, $p < 0.05$, Figure 2b). Further, balanopreputial separation occurs in *Mecp2*^{CD1}-null males at a lower body weight than WT controls ($t_{33} = 3.83$, $p < 0.001$; Figure 2b). Of note, and unlike the *Mecp2*-null males on B6.129 background, the testes of young adult *Mecp2*^{CD1}-null males were descended and visible, and showed no significant differences in weight (Student's t-test, $p > 0.05$, Figure 2d) or length (Student's t-test, $p > 0.05$, Figure 2e). Similar to in females, we did not find histological abnormalities in the gonads of pubescent male mice (Figure 2f), observing similar amount of spermatides (Figure 2g) and Leydig cells (Figure 2h) in both genotypes (Student's t-test, $p > 0.05$ in both cases).

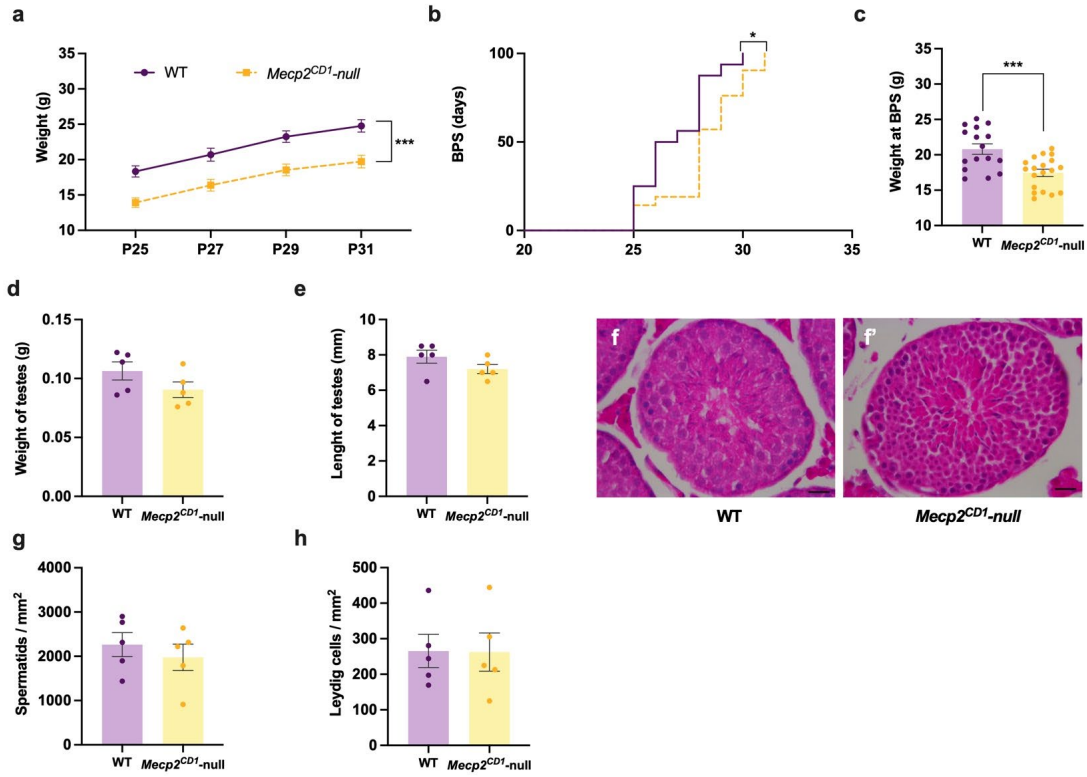

Figure 2. Weight gain and pubertal development in *Mecp2*^{CD1}-null male mice are significantly affected. a) Graphical representation of body weight gain in *Mecp2*^{CD1}-null males in comparison with their WT control mice. b) Days to balanopreputial separation (BPS) in WT and *Mecp2*^{CD1}-null males and c) weight at BPS. d) Length and e) weight of testes. Histological representative images of WT (f) and *Mecp2*^{CD1}-null (f') testes. g) Number of spermatides. h) Number of Leydig cells. Data are shown as Mean ± S.E.M. * $p < 0.05$; *** $p < 0.001$. Scale bar: 20µm

The density of GnRH neurons is increased in young adult *Mecp2*^{CD1}-null males

Subfertility and aberrant sexual development had been previously linked to the early loss of GnRH neurons in a mouse model of Trisomy 21 (36). Hence, we analysed the distribution and density of GnRH neurons in young adult mice. We found a low number of GnRH-immunoreactive (ir) neurons in the olfactory bulbs (Figure 3a), with no quantitative differences between genotypes in any sex (Figure 3b, c). As expected, the majority of GnRH neurons were mainly located in the septal area and the rostral hypothalamus (Bregma 0.5 to 0.02 mm) (37), both in males and females and in both genotypes (Figure 3d). Further, we corroborated that GnRH neurons co-expressed MeCP2 in WT mice (Supplementary Figure S4a), but, as expected, some GnRH neurons did not express this protein in *Mecp2*^{CD1}-het females (Supplementary Figure S4b). Quantitatively, and in agreement with the lack of effect on puberty onset of *Mecp2* mutation in heterozygosity in females, the density of GnRH neurons was not significantly different between *Mecp2*^{CD1}-het females and their WT controls (Student's t-test, $p > 0.05$, $p > 0.05$, Figure 3b and e) either in olfactory bulbs or in septo-hypothalamic levels. In contrast, we found an increase in GnRH neurons in *Mecp2*^{CD1}-null as compared to WT male mice ($t_{10} = 2.83$; $p = 0.018$, Figure 3f) specifically in the septo-hypothalamic area.

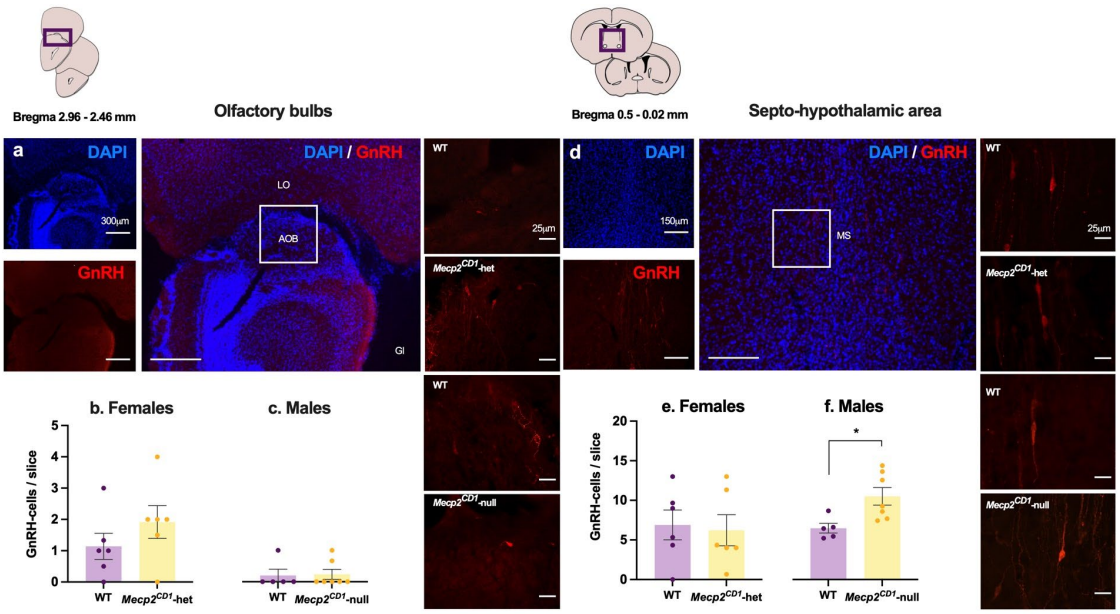

Figure 3. Septo-hypothalamic GnRH-positive cells are increased in *Mecp2*^{CD1}-null male mice. a) Representative images of GnRH immunofluoresecence in the olfactory bulbs, where these neurons were scarce both in females (b) and males (c), with no differences between genotypes. d) Representative images of GnRH immunofluorescence in the septo-hypothalamic area. Density of GnRH neurons was not statistically different between WT and *Mecp2*^{CD1}-het females (e), whereas the number of GnRH neurons was significantly increased in mutant males as compared to WT controls (f). Data are shown as Mean ± S.E.M. * $p < 0.05$. Scale bar: 50µm

387 **Circulating levels of reproductive hormones are reduced in young adult *Mecp2*^{CD1}-**
388 **null males**
389 Given the lack of significant effects of *Mecp2* in heterozygosity in females, we decided
390 to focus further experiments in males. We sought to analyse whether the excess of GnRH
391 neurons in *Mecp2*^{CD1}-null males could lead to increased levels of circulating hormones.
392 Surprisingly, we found that relative circulating levels of GnRH showed a trend toward
393 reduction in *Mecp2*^{CD1}-null as compared to WT males ($t_{12} = 2.08$; $p = 0.06$; Figure 4a).
394 Further, relative LH and testosterone levels were significantly lower in *Mecp2*^{CD1}-null
395 males compared to controls (Student's t test, $t_{26} = 2.17$, Figure 4b; $t_{21} = 2.33$, Figure 4c,
396 $p < 0.05$ in both cases).

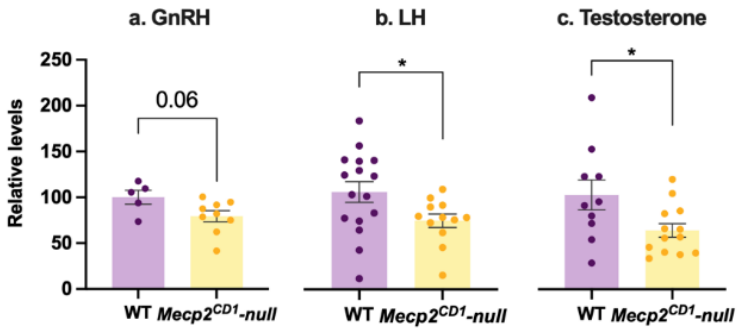

397
398 **Figure 4. Plasma levels of reproductive hormones in male mice.** a) GnRH; b) LH
399 and c) testosterone circulating levels were decreased in *Mecp2*^{CD1}-null male mice relative
400 to WT. Data are shown as Mean ± S.E.M. * $p < 0.05$
401
402 **Testosterone-dependent AVP-ergic innervation in the lateral habenula is reduced**
403 **in young adult *Mecp2*^{CD1}-null males**
404 In a previous study using *Mecp2*-null males on B6.129 background, we found
405 significantly decreased testosterone-dependent AVP-ergic innervation in those mice
406 (28). Here, we replicated this measure in *Mecp2*^{CD1}-null males, where AVP-ergic
407 innervation was almost absent in the lateral habenula of mutant males (Student's t-test,
408 $t_3 = 3.02$; $p < 0.05$, Figure 5d, e and f and Supplementary Figure S5a, b and b'). As in
409 our previous study, this reduction appears to be specific to testosterone-dependent
410 innervation, since the number of AVP cells in the paraventricular nucleus of the
411 hypothalamus is similar in *Mecp2*^{CD1}-null males and controls, thus not affected by
412 genotype (Student's t-test, $p > 0.05$; Figure 5 a, d , c; and Supplementary Figure S5c, d
413 and d').

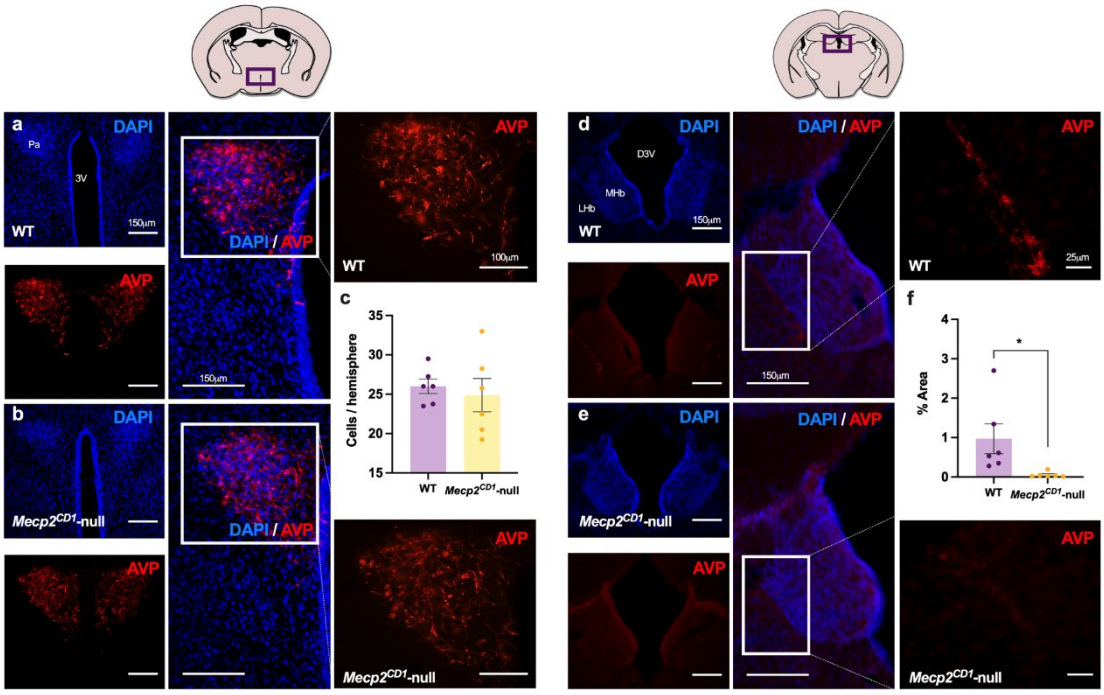

Figure 5. Vasopressinergic testosterone-dependent innervation is reduced in adult *Mecp2*^{CD1}-null males. Representative images of the paraventricular nucleus of the hypothalamus (Pa, Bregma -0.58mm) in a WT (a) and a *Mecp2*^{CD1}-null male (b). The density of AVP-ergic neurons is not affected by genotype (c). By contrast, representative images of the testosterone-dependent innervation of the lateral habenula (LHb, Bregma -1.58mm) in a WT (d) and *Mecp2*^{CD1}-null male (e) show a strongly reduced density of neuronal fibres in mutant animals (f). Data are shown as Mean ± S.E.M. * $p < 0.05$. Scale bar: 50µm

Discussion

In this work, we sought to study pubertal dysregulation in RTT syndrome using a mouse model deficient for *Mecp2*, derived to the CD1 strain to improve reproductive capacity. Whereas in heterozygous females we did not find significant effects on pubertal development, we found a significant delay in achieving pubertal milestones in *Mecp2*^{CD1}-null males as compared to their WT counterparts, a delay that may be influenced by the significantly lower weight during infancy and pubescence in these males. Further, we found an excess of GnRH neurons in the septo-hypothalamic region in young adult *Mecp2*^{CD1}-null males, contrasting with lower circulating levels of LH and testosterone, suggesting a dysregulation of the hypothalamic-pituitary-gonadal axis.

Although RTT syndrome is defined as a neurodevelopmental disorder, it is in fact a multiorgan disease affecting multiple systems in the body, causing gastrointestinal and orthopaedic problems, altered immune response and endocrine comorbidities (38–40). The most common symptoms related to endocrine dysfunction are low bone mineral

438 content, malnutrition (which could be also related to motor impairment causing difficulties
439 in eating) and alterations in the initiation of puberty (9,38,40,41). With regards to puberty
440 timing, data are scarce and conflicting. Various longitudinal population-based studies
441 suggest that a subset of patients with RTT (3-6%) experience premature menarche
442 (9,42), particularly those with milder mutations in the *MECP2* gene (9). In contrast, 19%
443 of girls were found to experience a delayed menarche (9). Overall, data from human
444 patients with RTT suggest that the disease is associated with deviations from normal
445 pubertal timing, with some patients experiencing early puberty onset, premature
446 thelarche but delayed menarche (9) .
447 Body weight and nutrition have a strong influence on pubertal timing and reproductive
448 health (43), and both patients with RTT and the mouse model studied here are likely to
449 be affected by these factors. Indeed, *Mecp2*^{CD1}-null males showed a significantly lower
450 weight than healthy controls at all stages, and a significantly delayed balanopreputial
451 separation, which occurred at lower body weight, in comparison to WT males.
452 By contrast, in our cohort of *Mecp2*^{CD1}-het females, body weight was, overall, not
453 significantly different from WT controls, and neither were vaginal opening or first
454 oestrous, a measure which more accurately reflects the onset of human puberty.
455 Thus, early onset of the disease in males, in which the complete loss of *Mecp2* strongly
456 affects most phenotypes (28,44) and reduces the lifespan of these mice (25), producing
457 low weight and ill health, might have a profound influence on pubertal development in
458 mutant males. Since the onset of symptoms in *Mecp2*-het mice is delayed and more
459 variable than in males (25), with some females being asymptomatic even by 5 months
460 of age (27), future studies should investigate pubertal development in a larger cohort of
461 female mice, following their symptoms into older adulthood.
462 The hypothalamic GnRH neurons are key regulators of gonadal hormones and hence of
463 pubertal onset and fertility. Previous reports have shown hypothalamic dysfunction in
464 *Mecp2*-mutant mice, including in the hypothalamic-hypophyseal-adrenal axis (8,45); and
465 in leptin pathways (46,47). Indeed, a recent report studying *Mecp2*-mutant mice showed
466 that, whereas the growth of most brain areas (such as neocortex and hippocampus) is
467 delayed in males and females, this growth is completely arrested in the hypothalamus,
468 suggesting a more severe impairment of this important neuroendocrine structure (48).
469 However, to our knowledge, our study is the first to report an increased density of GnRH
470 neurons in the septo-hypothalamic region in *Mecp2*^{CD1}-null males. Excess of
471 hypothalamic GnRH neurons due to enhanced survival and migration was demonstrated
472 following deletion of neuropilin-1 in GnRH neurons in a mouse model of central
473 precocious puberty (49).

474 The increased number of GnRH neurons in *Mecp2*^{CD1}-null males, however, did not lead
475 to increased GnRH circulating content, but rather a slightly lower concentration of this
476 hormone. In addition, we found significantly lower circulating levels of both LH and
477 testosterone in *Mecp2*^{CD1}-null males, in agreement with a previous study (28). Several
478 mechanisms might explain this finding. As described, the low body weight of these males
479 may have led to delayed puberty with hypogonadism. In circumstances of low nutrition
480 and chronic disease, GnRH pulsatility is impaired, with consequent functional
481 hypogonadotropic hypogonadism and thus delayed pubertal onset. It is conceivable that
482 loss of *Mecp2* might result in increased hypothalamic GnRH neurons, but functional
483 hypogonadism secondary to the whole-body effects of *Mecp2* deficiency might overcome
484 this, meaning that instead of precocious puberty, a phenotype of delayed puberty is seen
485 in this model. In keeping with this, it is interesting that *Mecp2*^{CD1}-null males show pubertal
486 onset at a lower body weight than healthy males.
487 In terms of the mechanism by which loss of *Mecp2* could affect GnRH neurons, this might
488 occur through a dysregulation of Erα signaling, which is regulated by MeCP2 (24). The
489 loss of *Mecp2* could also affect cells upstream of GnRH, for example, via arcuate nucleus
490 kisspeptin modulation of GnRH release. As described, MECP2 colocalises with the
491 histone mark H3K27me3. Enhanced H3K27me3 content at the 5′ regulatory region of
492 the Kiss1 gene silences its expression (20), whilst reduction leads to increased *Kiss1*
493 expression, GnRH pulsatility and pubertal development. Male mice with disrupted *Kiss1*
494 expression show a reduction in testis size as well as lower levels of testosterone (50).
495 Additionally, a study using a mouse model of *MECP2* duplication syndrome found that
496 circulating levels of testosterone were increased in these mice (51). In these mice, it was
497 shown that *Mecp2* was expressed in Leydig cells and led to an increase of androgen
498 synthesis via an upregulation of the receptor for LH (LHCGR) and a reduction in
499 aromatization to produce oestrogens (51). Although we did not find visible alterations in
500 Leydig cells in our samples, future studies should address whether *Mecp2*^{CD1}-null males
501 display lower levels of LHR in these cells. Finally, the lower levels of LH found in these
502 mice would contribute to a lesser stimulation of Leydig cells, leading to the observed
503 lower levels of testosterone.
504 In female mice, however, we did not find significant differences in number of GnRH cells.
505 As with pubertal timing, the later onset of symptoms in *Mecp2*^{CD1}-het females might
506 explain this difference. Further, since the MeCP2 protein is expressed in the nucleus of
507 GnRH neurons, skewed X inactivation in these cells could contribute to different
508 outcomes in terms of symptoms (52,53) and pubertal timing. Future studies assessing
509 the GnRH system and circulating levels of GnRH, LH and sex steroids in older females
510 might reveal relevant alterations.

511 The effects of pubertal dysregulation and altered hormonal signalling have an influence
512 beyond the reproductive axis. Thus, brain circuits dependent on the levels of sex steroid
513 hormones, such as the AVP-ergic system in males, display an aberrant configuration in
514 *Mecp2*-null males, as seen previously (28) and in the present study. These circuits
515 are involved in the control of emotional and social behaviour (54,55), highlighting the
516 necessity of further investigating the mechanism by which *Mecp2* deficiency may impact
517 their wiring, with the aim of finding novel therapeutic targets to potentially ameliorate
518 emotional and social impairment in RTT and related conditions.

519 **Limitations**

520 Despite the high validity of the model, there are still a number of concerns when trying
521 to translate animal data to humans. For example, in humans, boys usually die perinatally,
522 and females develop the first symptoms during early infancy, whereas in mice, males
523 display an overt phenotype around adolescence and females after young adulthood
524 (25,27). Hence, the biological age of the animals and humans in terms of
525 symptomatology is not comparable. Second, the pubertal markers used in the mouse do
526 not completely match those of humans. In spite of these limitations, our data in the mouse
527 model supports a disruption of the hypothalamic-pituitary-gonadal axis caused by *Mecp2*
528 deficiency, whose mechanism warrants further investigation.

529 **Conclusions**

530 In this study, we found that a mouse model deficient for *Mecp2* display reduction in body
531 weight during pubescence and dysregulated pubertal timing and function of the
532 hypothalamic-pituitary-gonadal axis. The effects found are strongly significant in males,
533 hemizygous for the mutation. By contrast, we did not find significant differences in
534 females, which could be related to heterozygosity leading to variable symptom onset.
535 Further, we found a significant increase in GnRH neurons but a decrease in circulating
536 GnRH, LH and testosterone in males, suggesting a general malfunction of the
537 hypothalamic-hypophyseal-gonadal axis. Since pubertal dysregulation has been
538 observed in human patients with mutations in *MECP2*, our study can be used as a
539 starting point to further investigate the biological mechanism by which *MECP2*
540 dysfunction contributes to alterations in puberty.

541

542 **List of abbreviations**

AVP	Arginine-vasopressin
BPS	Balanopreputial separation

CPP	Central precocious puberty
DAPI	4’,6- diamino-2-fe-niindol
ERβ	Estrogen receptor-β
FSH	Follicle stimulant hormone
FXYD1	FXYD domain-containing transport regulator 1
GnRH	Gonadotropin Realising Hormone
LH	Luteinizing hormone
LHb	Lateral habenula
LHR	Receptor for LH
MDS	MECP2 duplication syndrome
MECP2	Methyl CpG-binding protein 2
NDS	Normal donkey serum
Pa	Paraventricular nucleus
PBS	Phosphate saline solution
PFA	Parafolmaldehyde
RTT	Rett syndrome
TBS	TRIS buffered saline
VO	Vaginal opening

545 **References**

546 1. Nan X, Campoy FJ, Bird A. MeCP2 is a transcriptional repressor with abundant
547 binding sites in genomic chromatin. Cell. 1997;88(4):471–81. doi:10.1016/S0092-
548 8674(00)81887-5 PubMed PMID: 9038338.
549 2. Chahrour M, Sung YJ, Shaw C, Zhou X, Wong STC, Qin J, et al. MeCP2, a key
550 contributor to neurological disease, activates and represses transcription. Science
551 (1979). 2008;320(5880):1224–9. doi:10.1126/science.1153252 PubMed PMID:
552 18511691.
553 3. Shahbazian MD, Antalffy B, Armstrong DL, Zoghbi HY. Insight into Rett
554 syndrome: MeCP2 levels display tissue- and cell-specific differences and correlate with
555 neuronal maturation. Hum Mol Genet. 2002 Jan 15;11(2):115–24.
556 doi:10.1093/hmg/11.2.115 PubMed PMID: 11809720.
557 4. Smrt RD, Eaves-Egenes J, Barkho BZ, Santistevan NJ, Zhao C, Aimone JB, et
558 al. Mecp2 deficiency leads to delayed maturation and altered gene expression in
559 hippocampal neurons. Neurobiol Dis. 2007;27(1):77–89. doi:10.1016/j.nbd.2007.04.005
560 PubMed PMID: 17532643.
561 5. Moretti P, Zoghbi HY. MeCP2 dysfunction in Rett syndrome and related
562 disorders. Current Opinion in Genetics and Development. 2006.
563 doi:10.1016/j.gde.2006.04.009
564 6. Amir RE, Van den Veyver IB, Wan M, Tran CQ, Francke U, Zoghbi HY. Rett
565 syndrome is caused by mutations in X-linked MECP2, encoding methyl- CpG-binding
566 protein 2. Nature Genet. 1999;23(2):185–8. doi:10.1038/13810 PubMed PMID:
567 10508514.
568 7. Lombardi LM, Baker SA, Zoghbi HY. MECP2 disorders: From the clinic to mice
569 and back. Journal of Clinical Investigation. 2015. p. 2914–23. doi:10.1172/JCI78167
570 PubMed PMID: 26237041.
571 8. Abellán-Álvaro M, Stork O, Agustín-Pavón C, Santos M. MeCP2 haplodeficiency
572 and early-life stress interaction on anxiety-like behavior in adolescent female mice. J
573 Neurodev Disord. 2021;13(1):59. doi:10.1186/s11689-021-09409-7 PubMed PMID:
574 34895132.
575 9. Killian JT, Lane JB, Cutter GR, Skinner SA, Kaufmann WE, Tarquinio DC, et al.
576 Pubertal Development in Rett Syndrome Deviates From Typical Females. Pediatr
577 Neurol. 2014 Dec;51(6):769–75. doi:10.1016/j.pediatrneurol.2014.08.013
578 10. Tsuji-Hosokawa A, Matsuda N, Kurosawa K, Kashimada K, Morio T. A Case of
579 MECP2 Duplication Syndrome with Gonadotropin-Dependent Precocious Puberty. Horm
580 Res Paediatr. 2017;87(4):271–6. doi:10.1159/000449222 PubMed PMID: 27649574.

11. Holm VA. Rett syndrome: a case report from an audiovisual program. Brain Dev. 1985;7(3):297–9. doi:10.1016/s0387-7604(85)80031-0 PubMed PMID: 4061761.

12. Baş VN, Çetinkaya S, Ağladıoğlu SY, Aksoy A, Gülpınar B, Aycan Z. Report of the first case of precocious puberty in Rett syndrome. J Pediatr Endocrinol Metab. 2013;26(9–10):937–9. doi:10.1515/jpem-2012-0418 PubMed PMID: 23612537.

13. Canton APM, Tinano FR, Guasti L, Montenegro LR, Ryan F, Shears D, et al. Rare variants in the MECP2 gene in girls with central precocious puberty: a translational cohort study. Lancet Diabetes Endocrinol. 2023 Aug;11(8):545–54. doi:10.1016/S2213-8587(23)00131-6

14. Canton APM, Mebarak JB, Read JE, Roberts SA, Benson M, Shenoy R, et al. MECP2 Rare Variants in Boys With Central Precocious Puberty. J Clin Endocrinol Metab. 2026 Oct 25;111(4). doi:10.1210/CLINEM/DGAF572 PubMed PMID: 41139199.

15. Lopez-Rodriguez D, Franssen D, Heger S, Parent AS. Endocrine-disrupting chemicals and their effects on puberty. Best Pract Res Clin Endocrinol Metab. 2021 Sep;35(5):101579. doi:10.1016/j.beem.2021.101579

16. Avendaño MS, Vazquez MJ, Tena-Sempere M. Disentangling puberty: novel neuroendocrine pathways and mechanisms for the control of mammalian puberty. Hum Reprod Update. 2017 Nov 1;23(6):737–63. doi:10.1093/humupd/dmx025

17. Campbell RE, Coolen LM, Hoffman GE, Hrabovszky E. Highlights of neuroanatomical discoveries of the mammalian gonadotropin-releasing hormone system. J Neuroendocrinol. 2022 May 3. doi:10.1111/jne.13115

18. Deng V, Matagne V, Banine F, Frerking M, Ohliger P, Budden S, et al. FXYD1 is an MeCP2 target gene overexpressed in the brains of Rett syndrome patients and Mecp2 -null mice. Hum Mol Genet. 2007 Mar 15;16(6):640–50. doi:10.1093/hmg/ddm007

19. Garcia-Rudaz C, Deng V, Matagne V, Ronnekleiv OK, Bosch M, Han V, et al. FXYD1, a Modulator of Na + ,K + -ATPase Activity, Facilitates Female Sexual Development by Maintaining Gonadotrophin-Releasing Hormone Neuronal Excitability. J Neuroendocrinol. 2009 Feb;21(2):108–22. doi:10.1111/j.1365-2826.2008.01812.x

20. Diotel N, Mérot Y, Coumailleau P, Gueguen M, Sérandour AA, Salbert G, et al. 5-hydroxymethylcytosine marks postmitotic neural cells in the adult and developing vertebrate central nervous system. Journal of Comparative Neurology. 2017 Feb 15;525(3):478–97. doi:10.1002/cne.24077

21. Lee W, Kim J, Yun JM, Ohn T, Gong Q. MeCP2 regulates gene expression through recognition of H3K27me3. Nat Commun. 2020 Jun 19;11(1):3140. doi:10.1038/s41467-020-16907-0

616 22. Mellén M, Ayata P, Dewell S, Kriaucionis S, Heintz N. MeCP2 Binds to 5hmC
617 Enriched within Active Genes and Accessible Chromatin in the Nervous System. Cell.
618 2012 Dec;151(7):1417–30. doi:10.1016/j.cell.2012.11.022
619 23. Herbison AE, Pape JR. New Evidence for Estrogen Receptors in Gonadotropin-
620 Releasing Hormone Neurons. Front Neuroendocrinol. 2001 Oct;22(4):292–308.
621 doi:10.1006/frne.2001.0219
622 24. Westberry JM, Trout AL, Wilson ME. Epigenetic regulation of estrogen receptor
623 α gene expression in the mouse cortex during early postnatal development.
624 Endocrinology. 2010. doi:10.1210/en.2009-0955
625 25. Guy J, Hendrich B, Holmes M, Martin JE, Bird a. A mouse Mecp2-null mutation
626 causes neurological symptoms that mimic Rett syndrome. Nat Genet. 2001;27(3):322–
627 6. doi:10.1038/85899 PubMed PMID: 11242117.
628 26. Picker JD, Yang R, Ricceri L, Berger-Sweeney J. An altered neonatal behavioral
629 phenotype in Mecp2 mutant mice. Neuroreport. 2006 Apr;17(5):541–4.
630 doi:10.1097/01.WNR.0000208995.38695.2F PubMed PMID: 16543822.
631 27. Cuitavi J, Martínez-Rodríguez E, Abellán-Álvaro M, García-Arencibia M, Santos
632 M, Hipólito L, et al. Longitudinal Analysis in Mecp2-het Female Mice Reveals Atypical
633 Nociceptive Behaviours. ResearchSquare; 2025. doi:10.21203/rs.3.rs-5804567/v1
634 28. Martínez-Rodríguez E, Martín-Sánchez A, Kul E, Bose A, Martínez-Martínez FJ,
635 Stork O, et al. Male-specific features are reduced in Mecp2-null mice: analyses of
636 vasopressinergic innervation, pheromone production and social behaviour. Brain Struct
637 Funct. 2020 Sep 4;225(7):2219–38. doi:10.1007/s00429-020-02122-6 PubMed PMID:
638 32749543.
639 29. Cobolli Gigli C, Scaramuzza L, Gandaglia A, Bellini E, Gabaglio M, Parolaro D,
640 et al. MeCP2 Related Studies Benefit from the Use of CD1 as Genetic Background. PLoS
641 One. 2016;11(4):e0153473. doi:10.1371/journal.pone.0153473 PubMed PMID:
642 27097329.
643 30. Tuttle AH, Philip VM, Chesler EJ, Mogil JS. Comparing phenotypic variation
644 between inbred and outbred mice. Nat Methods. 2018 Dec 1;15(12):994–6.
645 doi:10.1038/S41592-018-0224-7 PubMed PMID: 30504873.
646 31. Arellano JI, Duque A, Rakic P. A coming-of-age story: adult neurogenesis or
647 adolescent neurogenesis in rodents? Front Neurosci. 2024 Mar 5;18.
648 doi:10.3389/fnins.2024.1383728
649 32. Quignon C. Collection and Analysis of Vaginal Smears to Assess Reproductive
650 Stage in Mice. Curr Protoc. 2023 Sep 19;3(9). doi:10.1002/cpz1.887

33. Ajayi AF, Akhigbe RE. Staging of the estrous cycle and induction of estrus in experimental rodents: an update. Fertil Res Pract. 2020 Dec 14;6(1):5. doi:10.1186/s40738-020-00074-3

34. Brust V, Schindler PM, Lewejohann L. Lifetime development of behavioural phenotype in the house mouse (Mus musculus). Front Zool. 2015 Dec 24;12(S1):S17. doi:10.1186/1742-9994-12-S1-S17

35. Cobolli Gigli C, Scaramuzza L, Gandaglia A, Bellini E, Gabaglio M, Parolaro D, et al. MeCP2 related studies benefit from the use of CD1 as genetic background. PLoS One. 2016 Apr 1;11(4). doi:10.1371/journal.pone.0153473 PubMed PMID: 27097329.

36. Manfredi-Lozano M, Leysen V, Adamo M, Paiva I, Rovera R, Pignat JM, et al. GnRH replacement rescues cognition in Down syndrome. Science. 2022;377(6610):eabq4515. doi:10.1126/science.abq4515 PubMed PMID: 36048943.

37. Paxinos G, Franklin K. Academic Press [Internet]. 2012. p. 360 p. Paxinos and Franklin's the Mouse Brain in Stereotaxic Coordinates. Available from: https://www.elsevier.com/books/paxinos-and-franklins-the-mouse-brain-in-stereotaxic-coordinates/paxinos/978-0-12-391057-8

38. Pepe G, Coco R, Corica D, Luppino G, Morabito LA, Lugarà C, et al. Endocrine disorders in Rett syndrome: a systematic review of the literature. Front Endocrinol (Lausanne). 2024 Oct 31;15. doi:10.3389/fendo.2024.1477227

39. De Felice C, Leoncini S, Signorini C, Cortelazzo A, Rovero P, Durand T, et al. Rett syndrome: An autoimmune disease? Autoimmun Rev. 2016 Apr;15(4):411–6. doi:10.1016/j.autrev.2016.01.011

40. Wong LC, Chen Y, Tsai S, Lin Y, Hsu C, Wang H, et al. Dietary intake and growth deficits in Rett syndrome—A cross-section study. Autism Research. 2021 Jul 31;14(7):1512–21. doi:10.1002/aur.2508

41. Roende G, Petersen J, Ravn K, Fuglsang K, Andersen H, Nielsen JB, et al. Low bone turnover phenotype in Rett syndrome: results of biochemical bone marker analysis. Pediatr Res. 2014 Apr 27;75(4):551–8. doi:10.1038/pr.2013.252

42. Knight O, Bebbington A, Siafarikas A, Woodhead H, Girdler S, Leonard H. Pubertal trajectory in females with Rett syndrome: A population-based study. Brain Dev. 2013 Nov;35(10):912–20. doi:10.1016/j.braindev.2012.11.007

43. Tarquinio DC, Motil KJ, Hou W, Lee HS, Glaze DG, Skinner SA, et al. Growth failure and outcome in Rett syndrome. Neurology. 2012 Oct 16;79(16):1653–61. doi:10.1212/WNL.0b013e31826e9a70

44. Martínez-Rodríguez E, Martín-Sánchez A, Coviello S, Foiani C, Kul E, Stork O, et al. Lack of MeCP2 leads to region-specific increase of doublecortin in the olfactory

687 system. Brain Struct Funct. 2019 May 28;224(4):1647–58. doi:10.1007/s00429-019-
688 01860-6
689 45. Braun S, Kottwitz D, Nuber UA. Pharmacological interference with the
690 glucocorticoid system influences symptoms and lifespan in a mouse model of Rett
691 syndrome. Hum Mol Genet. 2012;21(8):1673–80. doi:10.1093/hmg/ddr602 PubMed
692 PMID: 22186023.
693 46. Torres-Andrade R, Moldenhauer R, Gutierrez-Bertín N, Soto-Covasich J,
694 Mancilla-Medina C, Ehrenfeld C, et al. The increase in body weight induced by lack of
695 methyl CpG binding protein-2 is associated with altered leptin signalling in the
696 hypothalamus. Exp Physiol. 2014 Sep 29;99(9):1229–40.
697 doi:10.1113/expphysiol.2014.079798
698 47. Wang X, Lacza Z, Sun YE, Han W. Leptin resistance and obesity in mice with
699 deletion of methyl-CpG-binding protein 2 (MeCP2) in hypothalamic pro-opiomelanocortin
700 (POMC) neurons. Diabetologia. 2014 Jan 28;57(1):236–45. doi:10.1007/s00125-013-
701 3072-0
702 48. Carli S, Chaabane L, De Rocco G, Albizzati E, Sormonta I, Calligaro S, et al. A
703 comprehensive longitudinal study of magnetic resonance imaging identifies novel
704 features of the Mecp2 deficient mouse brain. Neurobiol Dis. 2023 May;180:106083.
705 doi:10.1016/j.nbd.2023.106083
706 49. Vanacker C, Trova S, Shruti S, Casoni F, Messina A, Croizier S, et al. Neuropilin-
707 1 expression in GnRH neurons regulates prepubertal weight gain and sexual attraction.
708 EMBO J. 2020 Oct 5;39(19). doi:10.15252/embj.2020104633
709 50. d'Anglemont de Tassigny X, Fagg LA, Dixon JPC, Day K, Leitch HG, Hendrick
710 AG, et al. Hypogonadotropic hypogonadism in mice lacking a functional *Kiss1* gene.
711 Proceedings of the National Academy of Sciences. 2007 Jun 19;104(25):10714–9.
712 doi:10.1073/pnas.0704114104
713 51. Wang YM, Wu Y, Zheng YF, Wang HY. MeCP2 duplication causes
714 hyperandrogenism by upregulating LHCGR and downregulating RORα. Cell Death Dis.
715 2021 Oct 25;12(11):999. doi:10.1038/s41419-021-04277-4
716 52. Mykins M, Layo-Carris D, Dunn LR, Skinner DW, McBryar AH, Perez S, et al.
717 Wild-type MECP2 expression coincides with age-dependent sensory phenotypes
718 in a female mouse model for Rett syndrome. J Neurosci Res. 2023 Aug 7;101(8):1236–
719 58. doi:10.1002/jnr.25190
720 53. Braunschweig D. X-Chromosome inactivation ratios affect wild-type MeCP2
721 expression within mosaic Rett syndrome and Mecp2-/+ mouse brain. Hum Mol Genet.
722 2004 Apr 28;13(12):1275–86. doi:10.1093/hmg/ddh142

723 54. Neumann I, Landgraf R. Balance of brain oxytocin and vasopressin: implications
724 for anxiety, depression, and social behaviors. Trends Neurosci. 2012;35(11):649–59.
725 55. Otero-García M, Agustín-Pavón C, Lanuza E, Martínez-García F. Distribution of
726 oxytocin and co-localization with arginine vasopressin in the brain of mice. Brain Struct
727 Funct. 2016 Sep 20;221(7):3445–73. doi:10.1007/s00429-015-1111-y
728

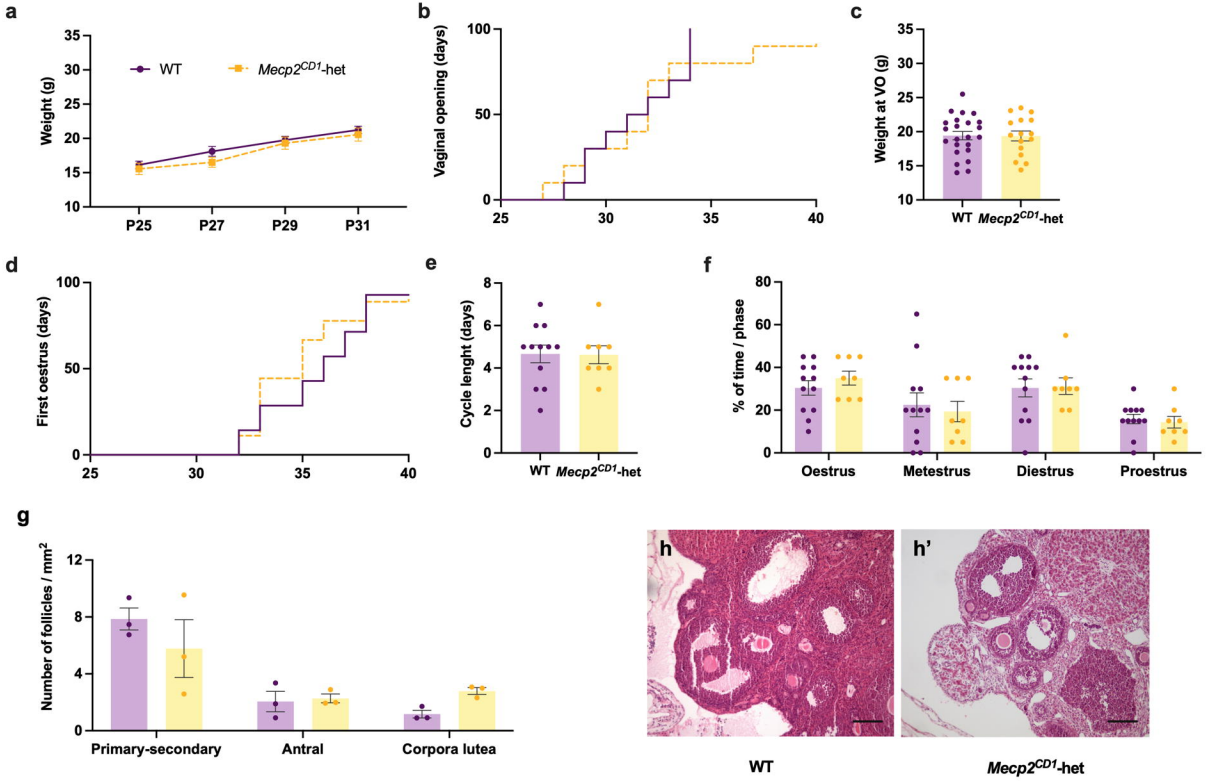
a
Weight (g)
35
30
25
20
15
10
WT
Mecp2CD1-het
P25
P27
P29
P31
b
Vaginal opening (days)
100
50
0
25
30
35
40
c
Weight at VO (g)
35
30
25
20
15
10
WT
Mecp2CD1-het
d
First oestrus (days)
100
50
0
25
30
35
40
e
Cycle lenght (days)
8
6
4
2
0
WT
Mecp2CD1-het
f
% of time / phase
80
60
40
20
0
Oestrus
Metestrus
Diestrus
Proestrus
g
Number of follicles / mm2
12
8
4
0
Primary-secondary
Antral
Corpora lutea
h
h'
WT
Mecp2CD1-het

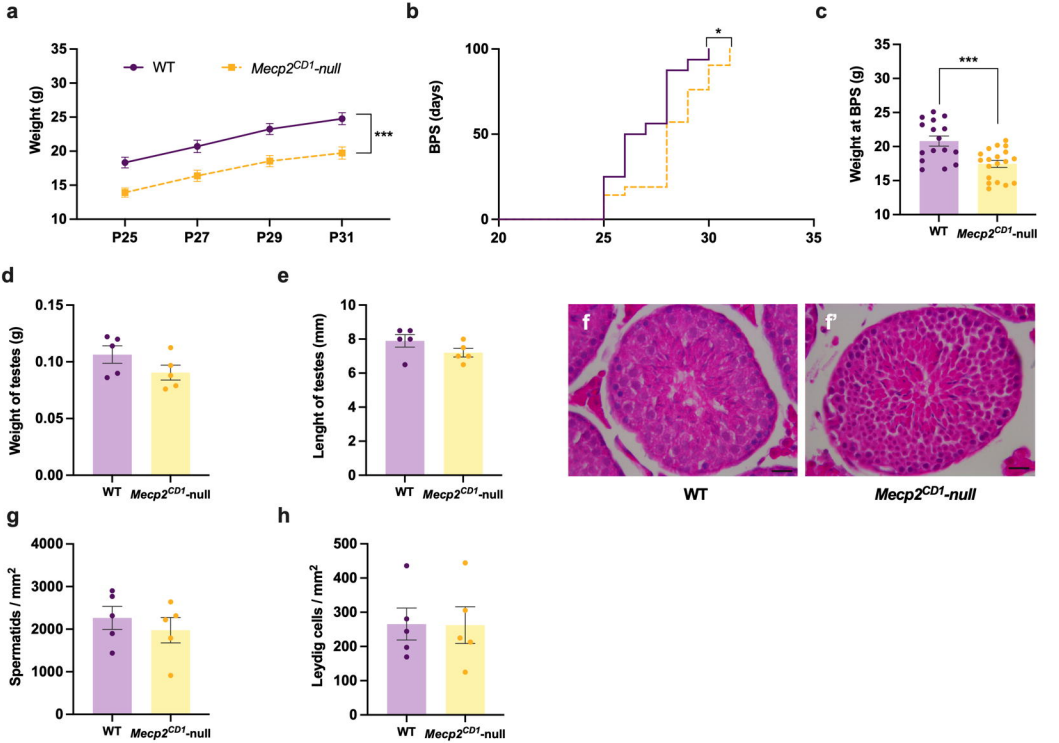
a
Weight (g)
35
30
25
20
15
10
WT
Mecp2CD1-null
***
P25
P27
P29
P31
b
BPS (days)
100
50
0
*
20
25
30
35
c
Weight at BPS (g)
35
30
25
20
15
10
***
WT
Mecp2CD1-null
d
Weight of testes (g)
0.15
0.10
0.05
0.00
WT
Mecp2CD1-null
e
Lenght of testes (mm)
10
8
6
4
2
0
WT
Mecp2CD1-null
f
f'
WT
Mecp2CD1-null
g
Spermatids / mm2
4000
3000
2000
1000
0
WT
Mecp2CD1-null
h
Leydig cells / mm2
500
400
300
200
100
0
WT
Mecp2CD1-null

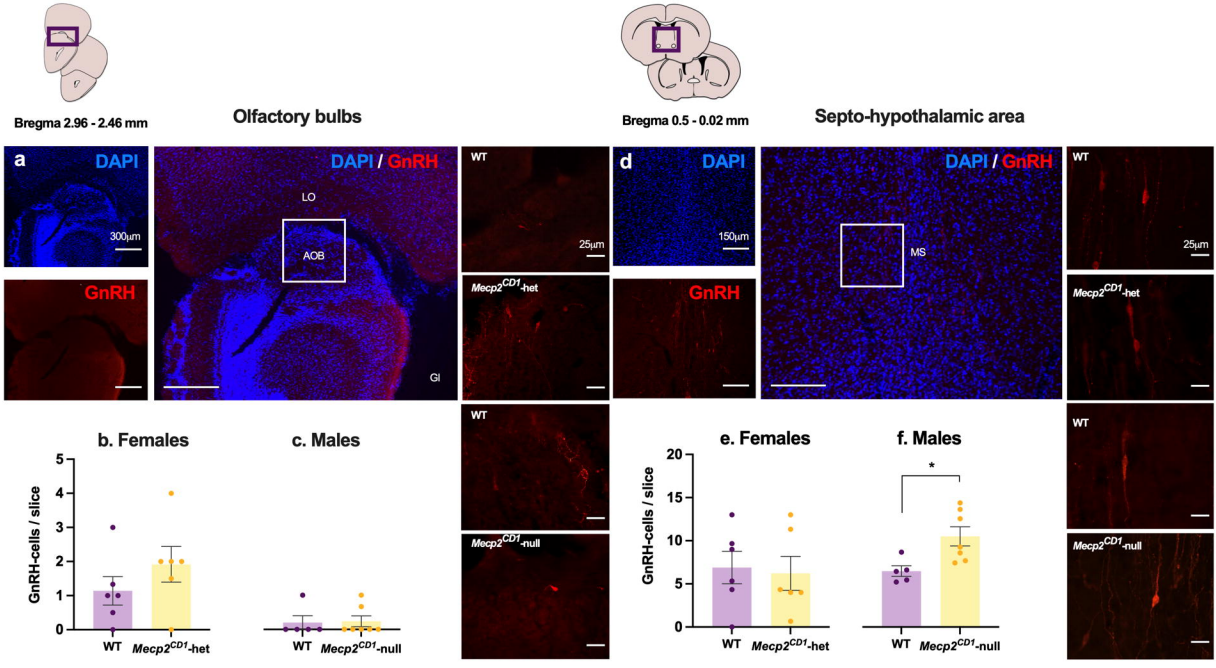
Bregma 2.96 - 2.46 mm
Olfactory bulbs
Bregma 0.5 - 0.02 mm
Septo-hypothalamic area
a
DAPI
300µm
GnRH
DAPI / GnRH
LO
AOB
GI
WT
25µm
Mecp2CD1-het
Mecp2CD1-null
d
DAPI
150µm
GnRH
DAPI / GnRH
MS
b. Females
c. Males
GnRH-cells / slice
WT
Mecp2CD1-het
Mecp2CD1-null
e. Females
f. Males
*

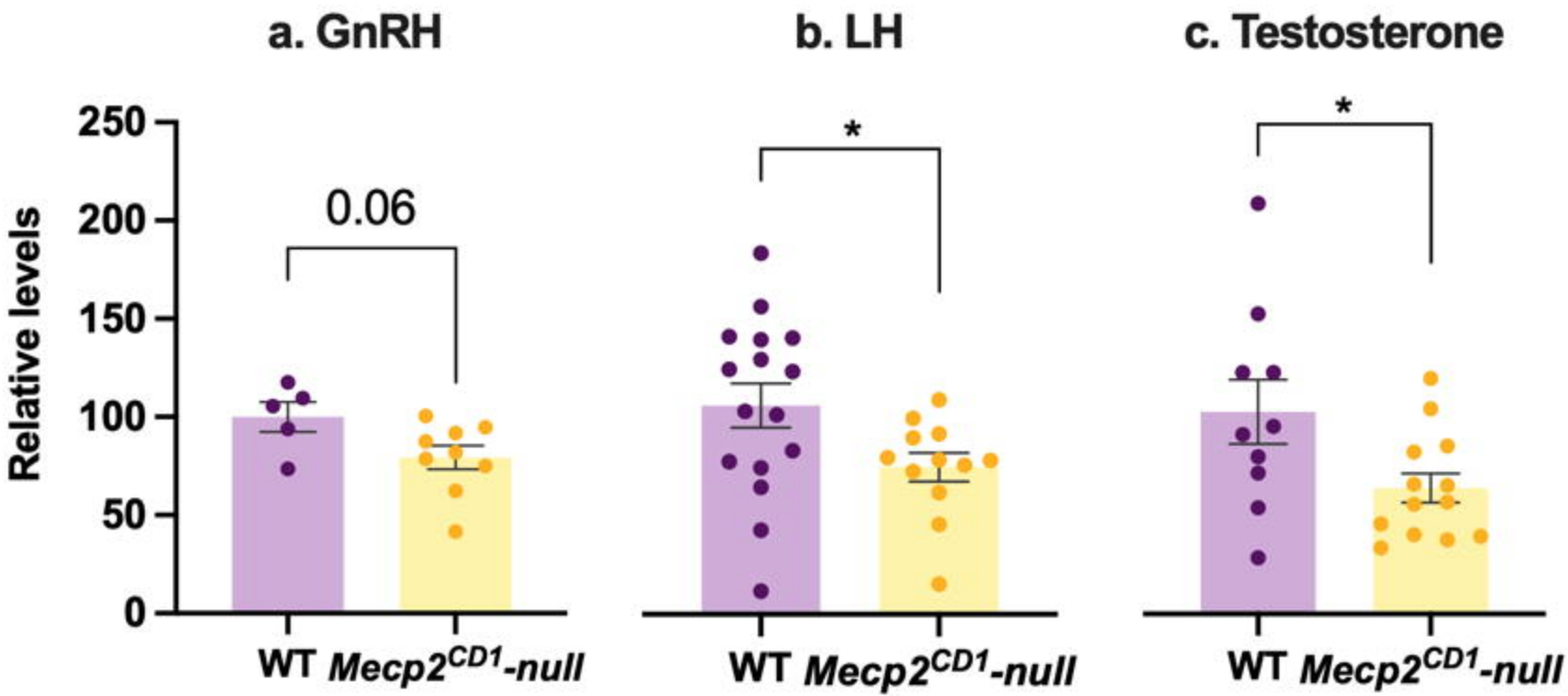
a. GnRH
b. LH
c. Testosterone
Relative levels
250
200
150
100
50
0
0.06
*
*
WT
Mecp2CD1-null
WT
Mecp2CD1-null
WT
Mecp2CD1-null

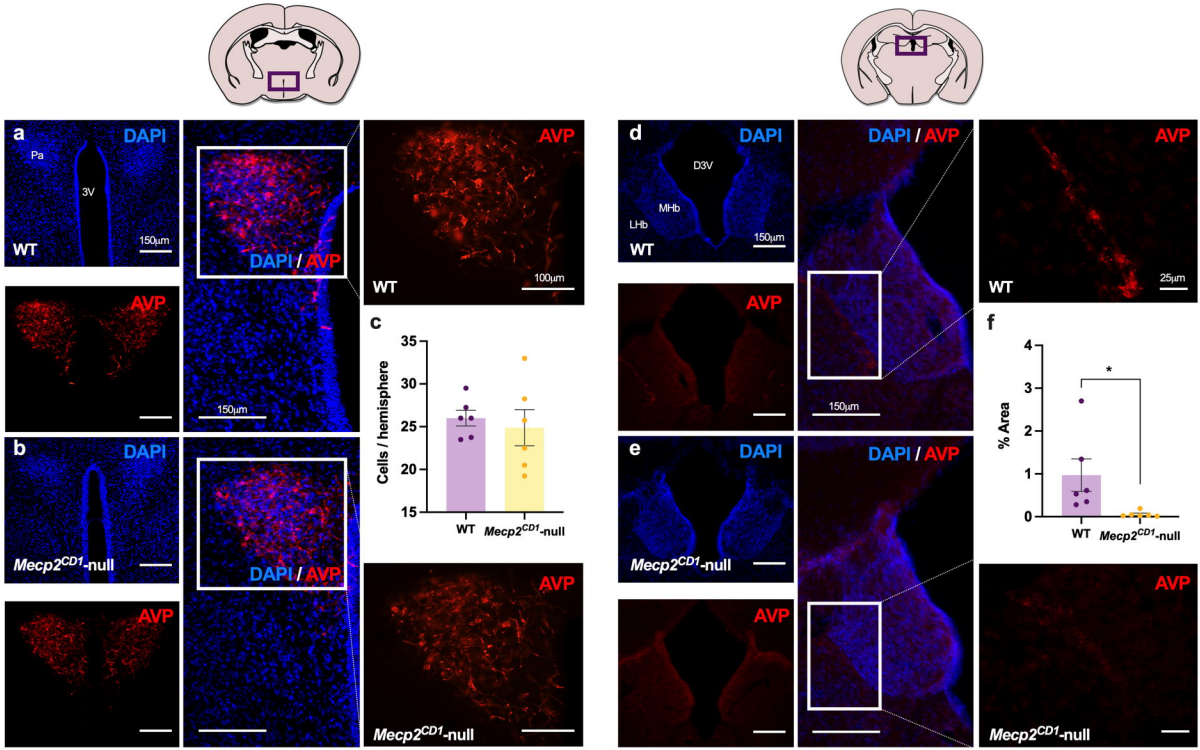
a
DAPI
Pa
3V
WT
150µm
AVP
DAPI / AVP
150µm
AVP
WT
100µm
b
DAPI
Mecp2CD1-null
AVP
DAPI / AVP
AVP
Mecp2CD1-null
c
Cells / hemisphere
35
30
25
20
15
WT
Mecp2CD1-null
d
DAPI
D3V
MHb
LHb
WT
150µm
AVP
DAPI / AVP
150µm
AVP
WT
25µm
e
DAPI
Mecp2CD1-null
AVP
DAPI / AVP
AVP
Mecp2CD1-null
f
% Area
4
3
2
1
0
*
WT
Mecp2CD1-null